Role of the S3-S4 Linker in *Shaker* Potassium Channel Activation

Rajesh Mathur, Jie Zheng, Yangyang Yan, and Fred J. Sigworth

From the Department of Cellular and Molecular Physiology, Yale University School of Medicine, New Haven, Connecticut 06520

ABSTRACT Structural models of voltage-gated channels suggest that flexibility of the S3-S4 linker region may be important in allowing the S4 region to undergo large conformational changes in its putative voltage-sensing function. We report here the initial characterization of 18 mutations in the S3-S4 linker of the *Shaker* channel, including deletions, insertions, charge changes, substitution of prolines, and chimeras replacing the 25-residue *Shaker* linker with 7- or 9-residue sequences from *Shab, Shaw*, or *Shal*. As measured in *Xenopus* oocytes with a two-microelectrode voltage clamp, each mutant construct yielded robust currents. Changes in the voltage dependence of activation were small, with activation voltage shifts of 13 mV or less. Substitution of linkers from the slowly activating *Shab* and *Shaw* channels resulted in a three- to fourfold slowing of activation and deactivation. It is concluded that the S3-S4 linker is unlikely to participate in a large conformational change during channel activation. The linker, which in some channel subfamilies has highly conserved sequences, may however be a determinant of activation kinetics in potassium channels, as previously has been suggested in the case of calcium channels.

KEY WORDS: potassium channel • mutagenesis • protein sequence • voltage clamp

INTRODUCTION

The high sensitivity of voltage-gated potassium and sodium channels arises from a large charge displacement, ~13 e_0 in magnitude, as a channel moves from its resting state to the open state (Schoppa et al., 1992; Hirschberg et al., 1995; Aggarwal and Mackinnon, 1996; Seoh et al., 1996). It is widely thought that this charge displacement involves the S4 region of the protein sequence, with contributions from other regions (Sigworth, 1994; Seoh et al., 1996). The S4 region of the *Shaker* potassium channel has seven basic residues which could contribute to the mobile charge, and recent experiments have shown changes in the accessibility of S4 residues upon voltage-dependent channel activation (Larsson et al., 1996; Yang et al., 1996). According to some theories, the S4 segment is an alpha helix that undergoes a large, helical screw movement normal to the lipid bilayer in order to transfer the necessary gating charge (Catterall, 1986; Durell et al. 1992). If indeed this is how the S4 region moves, then the S3-S4 linker, to which it is tethered at its NH_2-terminal end, must be flexible to support the large displacement.

There has been little study of the S3-S4 linker of voltage-gated channels, apart from work on L-type calcium channels by Nakai et al. (1994). These authors showed that exchange of the S3-S4 region in Domain 1 changed the channel from the skeletal muscle (slowly activating) to the cardiac (rapidly activating) kinetic behavior. A comparison of potassium channel S3-S4 linkers is shown in Fig. 1. The apparent length of the linker is variable between subfamilies, ranging from 25 residues for *Drosophila Shaker* to only 7 residues in *Shaw*. The members of the *Shaker* subfamily show a moderate degree of sequence identity, but within the *Shab* and *Shal* subfamilies there is a remarkable degree of identity between *Drosophila* and mammalian members, similar to the level of identity in the S4 regions. In the present study we investigate the role of the S3-S4 linker by asking how point mutations or major alterations in its sequence affect the voltage dependence and kinetics of activation gating in the *Shaker* K^+ channel.

MATERIALS AND METHODS

Site-directed Mutagenesis

Our constructs were based on ShΔ, a *Shaker* 29-4 cDNA clone (Kamb et al., 1988) having a deletion (Δ2-30) to remove fast inactivation (Hoshi et al. 1990). To better allow comparison with other reports in the literature, we adopt the residue numbering of the *Shaker* B splice variant (Schwarz et al, 1988), which differs from 29-4 at the NH_2 terminus and at four residues in the COOH-terminal region. The 2.1 kb ShΔ cDNA was subcloned at the EcoRI and HindIII restriction sites of pOEV (Pfaff et al, 1990). The LP-USE technique (Deng and Nickoloff, 1992; Ray and Nickoloff, 1992) was used for site-directed mutagenesis. In this technique a mutagenic and a selection primer are joined using PCR to obtain a single long primer for subsequent annealing with the denatured parental DNA and elongation with T4 polymerase. The mutagenic primers (synthesized at the DNA Synthesis Laboratory, Yale University) were 24–60 nucleotides in length, while the 24-mer selection primer changed the unique HindIII site to a MluI site. A PCR product of ~1.25 kb was generated using AmpliTaq DNA polymerase (Perkin Elmer Corp., Norwalk, CT) and separated from the unreacted primers by electrophore-

Dr. Mathur's present address is Cardiovascular Division, Brigham and Women's Hospital, 75 Francis St., Boston, MA 02115.

Address correspondence to Fred J. Sigworth, Department of Cellular and Molecular Physiology, Yale School of Medicine, 333 Cedar Street, New Haven, CT 06520-8026. Fax: 203-785-4951; E-mail: fred.sigworth@yale.edu

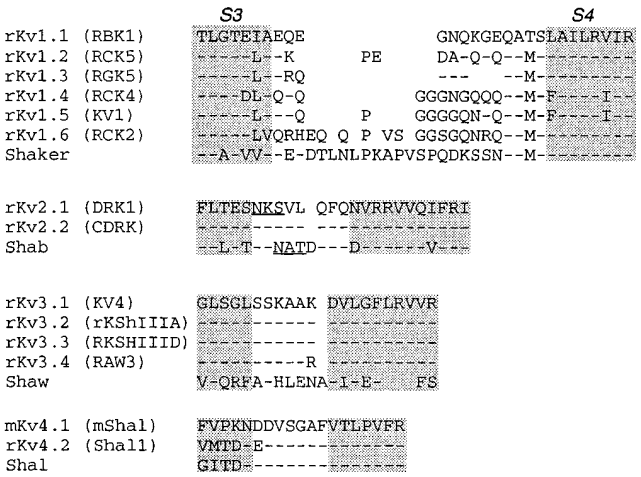

FIGURE 1. Alignment of the amino acid sequence of S3-S4 linkers in the K^+ channel subfamilies. Alignments of the protein coding sequences (Chandy and Gutman, 1994) were manually adjusted and are shown for the linker region across the four subfamilies. Sequences from rat (or mouse: *mKv4.1*) are compared with the corresponding *Drosophila* sequences. The start site of the linker in *Shaker* is taken to be E333 and the end S357 (Kamb et al., 1988; Schwarz et al., 1988); in the other subfamilies, the boundaries are as proposed by Butler et al. (1990). Within the *Shaker* subfamily, the rat linker sequence for a given member is identical to the corresponding frog, murine, bovine, and human sequences. In other subfamilies, fewer clones are described from different species, but the linkers are identical across all mammalian species reported. A conserved, potential N-glycosylation site in the *Shab* subfamily members is underlined. Dashes indicate amino acid residues identical to the sequence shown at the top of each group; blank spaces indicate gaps.

sis in low-melting 1% agarose gel. We used the Transformer Site-Directed Mutagenesis Kit (Clontech Laboratories, Palo Alto, CA) and the manufacturer's protocol to carry out the denaturation, annealing, elongation, ligation, and transformation steps into *Escherichia coli* strain BMH 71-18 mutS, which is defective in the mismatch repair function. Mutants were identified (blue colonies on X-gal/IPTG) by digestion with MluI restriction enzyme. The 1.25-kb PCR-generated segment in each positive mutant was completely sequenced (Sequenase Kit; U.S. Biochemical, Cleveland, OH). In a few cases, we obtained the desired mutant by direct colony transfer and hybridization with the respective mutagenic primer, using the ECL nonradioactive gene detection system (Amersham Corp., Arlington Heights, IL). The positive mutants were sequenced as stated above. The cDNAs were linearized with MluI (or EcoRV in some mutants obtained by the ECL system), and the capped, in vitro run-off T7 transcripts were synthesized and quantitated approximately by the intensity of ethidium bromide stained bands in 1% agarose (with 6% formaldehyde) gel. RNA was stored at −70°C.

Preparation of Oocytes and cRNA Injection

Harvested oocytes from *Xenopus laevis* were defolliculated by incubating with collagenase (type 1a; Sigma Chemical Co., St. Louis, MO) in OR3 medium (Blumenthal and Kaczmarek, 1992), which consisted of 50% Leibovitz's L-15 medium (Gibco BRL, Grand Island, NY), 15 mM HEPES, 5×10^4 U/liter Nystatin (Sigma Chemical Co.), 10 mg/liter Gentamycin (Sigma Chemical Co.), adjusted to pH 7.4. When the oocytes were well separated from each other (after ~2 h at room temperature), they were repeatedly washed with the OR3 medium to remove collagenase. Stage V and VI oocytes were sorted and maintained in OR3 medium at 20°C, before and after RNA injection. 50–100 nl of cRNA solution was injected into the vegetal pole of each oocyte. Concentrations of injected cRNAs were varied to control the level of expression.

Current Recordings

Oocytes were incubated for 2–6 d before recording currents from them at room temperature by two-microelectrode voltage-clamp (OC-725; Warner Instruments, New Haven, CT), using the Pulse software (HEKA-Electronic, Lambrecht, Germany) running on a Macintosh computer. Microelectrodes were filled with 1 M KCl and had resistances of 0.1 to 1 MΩ; a grounded shield between the electrodes reduced coupling capacitance. The standard bath solution was ND-96 (96 mM NaCl, 2 mM KCl, 1.8 mM $MgCl_2$, 1 mM $CaCl_2$, 5 mM HEPES, pH adjusted to 7.4). Bath electrodes were chlorided silver wires, except for experiments in which dithiothreitol was introduced into the bath, in which case a salt bridge was used. The current monitor signal was filtered with a 2 kHz Bessel filter and the linear leak and capacitative currents were subtracted by the P/4 method (Bezanilla and Armstrong, 1977) from a subtraction holding potential of −120 mV. The series resistance in the voltage-clamp system was estimated to be <200 Ω. For characterization of kinetics and activation, oocytes with currents at +70 mV in the range of 10–50 μA (mean 32 μA) were used.

Conductances were computed assuming a linear open-channel i-V relationship and a reversal potential of −80 mV, and normalized by the peak conductance (g_{max}) measured at +70 mV. Voltage dependence of activation was characterized by fitting to the fourth power of a Boltzmann function,

$$\frac{G}{G_{max}} = \frac{1}{[1 + e^{-k_a(V - V_a)}]^4}, \quad (1)$$

to obtain the steepness factor k_a and the midpoint voltage V_a.

Activation was characterized by a fit to the time course of the current elicited by depolarizations from a holding potential of −80 mV. The fit started near the time at which the current had reached 50% of maximum and ended at 50 ms. The fitting function was the sum of two exponential functions,

$$\frac{I_t}{I_0} = [A_1 e^{-t/\tau_{a1}} + A_2 e^{-t/\tau_{a2}}],$$

where I_t is the current at time t and I_o is the extrapolated value of the current at $t = 0$. The faster of the two time constants, τ_{a1}, always had the larger amplitude, >75% of the total amplitude at −30 mV and at 0 mV.

The time constants of current deactivation were obtained by fitting the currents following a 20-ms activating pulse to +40 mV, with a delay to allow instantaneous current changes to settle. The time course was fitted with the sum of two exponentials; the faster component τ_{d1}, which accounted for ~90% of the amplitude (from −80 to −20 mV) is shown in Fig. 7 and Table I. Time constant values from multiple determinations are reported as geometric means and SEM values.

RESULTS

Mutations in the Shaker S3-S4 Linker Do Not Affect Formation of Functional Channels

Fig. 2 summarizes the mutations that were made. The first five involved changes in the four contiguous acidic

TABLE I

Properties of Wild-type and S3-S4 Linker Mutants of the Shaker Channel

Channel	Activation τ_{a1} (ms) at −30 mV	Deactivation τ_{d1} (ms) at −60 mV	Activation voltage V_a (mV)	Activation slope (V)	Apparent gating valence (Z_{app})
Wild-type (ShΔ)	2.1 ± 0.2 (7)	1.0 ± 0.3 (6)	−38 ± 2 (5)	66 ± 4 (5)	6.0 ± 0.5 (5)
ΔE	1.6 ± 0.3 (6)	1.0 ± 0.2 (6)	−46 ± 5 (7)	77 ± 4 (7)	—
ΔEE	2.6 ± 0.4 (5)	0.8 ± 0.2 (4)	−45 ± 3 (7)	68 ± 6 (7)	—
ΔEEE	1.6 ± 0.6 (5)	1.3 ± 0.4 (4)	−49 ± 5 (5)	62 ± 5 (5)	5.5 ± 0.2 (6)
E→K	2.9 ± 0.4 (6)	0.7 ± 0.1 (6)	−45 ± 1 (5)	54 ± 2 (5)	—
EEED→KKKK	1.7 ± 0.2 (5)	1.0 ± 0.1 (5)	−33 ± 2 (6)	60 ± 3 (6)	5.6 ± 0.8 (8)
ΔA	3.4 ± 0.5 (7)	0.6 ± 0.1 (4)	−35 ± 2 (7)	70 ± 6 (7)	—
ΔM	1.5 ± 0.1 (6)	1.0 ± 0.1 (6)	−50 ± 2 (7)	62 ± 2 (7)	—
ΔAMS	3.6 ± 0.9 (5)	0.9 ± 0.2 (6)	−34 ± 2 (7)	82 ± 5 (7)	5.1 ± 0.4 (9)
P341A	2.3 ± 0.4 (6)	0.7 ± 0.1 (6)	−34 ±2 (7)	62 ± 4 (7)	5.3 ± 0.4 (6)
P344A	1.6 ± 0.1 (6)	0.8 ± 0.1 (5)	−37 ± 1 (7)	56 ± 2 (7)	—
P347A	2.2 ± 0.3 (6)	0.9 ± 0.1 (6)	−36 ± 1 (7)	60 ± 3 (7)	—
ShΔ/Cys	4.1 ± 0.5 (9)	1.2 ± 0.3 (9)	−32 ± 1 (4)	71 ± 3 (10)	—
ShΔ/FLAG	2.0 ± 0.2 (6)	0.6 ± 0.1 (5)	−37 ± 2 (7)	61 ± 4 (7)	—
ShΔ/HA	1.9 ± 0.2 (6)	0.6 ± 0.1 (6)	−34 ± 1 (6)	54 ± 3 (6)	5.2 ± 0.6 (7)
ShΔ/Xa	1.6 ± 0.3 (6)	0.7 ± 0.1 (6)	−39 ± 1 (4)	49 ± 4 (4)	—
ShΔ/Shab	6.3 ± 1.0 (6)	3.2 ± 0.6 (6)	−51 ± 1 (7)	86 ± 9 (7)	5.7 ± 0.5 (8)
ShΔ/Shaw	7.6 ± 1.6 (6)	1.8 ± 0.1 (6)	−31 ± 1 (10)	74 ± 4 (10)	5.3 ± 0.1 (8)
ShΔ/Shal	3.0 ± 0.6 (5)	0.6 ± 0.1 (6)	−28 ± 1 (6)	53 ± 2 (6)	4.7 ± 0.4 (7)

Values for the activation time constant τ_{a1} and deactivation time constant τ_{d1} are given as geometric mean ± SEM with the number of determinations in parentheses. Values for the activation midpoint voltage V_a, activation slope k_a, and apparent valence z_{app} are given as mean ± SD. Values of z_{app} were determined according to Eq. 2 at a potential where the conductance is 1% of the maximum value.

residues EEED at the NH_2-terminal end of the linker. Deletions of glutamate residues and charge reversals by replacement with lysines were performed. The second group of mutations involved deletions at the COOH-terminal end of the linker, where the AMS sequence is highly conserved within the *Shaker* subfamily. In the third group of mutations each of the proline residues in the S3-S4 region was changed to alanine, one at a time. The fourth group of mutations consisted of various insertions following P344. Insertions were a single cysteine residue or peptides 4–9 residues in length. The inserted sequences were influenza hemagglutinin (HA; Kast et al., 1995) and FLAG (Zhong et al., 1995) epitopes, and a Factor X_a cleavage-site sequence (Wearne, 1990). The fifth group were chimeric constructs, in which the *Shaker* linker was replaced with the shorter S3-S4 linkers from *Shab*, *Shaw*, and *Shal* genes.

The cRNAs bearing the various mutations were injected into *Xenopus laevis* oocytes, and the whole-oocyte K^+ currents were recorded by two-microelectrode voltage-clamp. Robust currents from each of the 18 mutants implied that none of mutations in the S3-S4 linker affected the synthesis and assembly of the functional *Shaker* K^+ channels in oocyte membranes.

Mutation Effects on Activation and Deactivation

Changes in channel activation due to the mutations were assayed using depolarizations and a deactivation protocol as shown in Fig. 3. Activation was characterized by the voltage dependence of steady-state conductance and an activation time constant. Starting at the time at which the current reaches 50% of its final value, the activation time course was fitted to the sum of two exponentials. The time constant τ_{a1} of the faster exponential was taken to be a measure of the activation kinetics, since the slower exponential had a small and variable amplitude, always <25% of the total. Deactivation was similarly characterized by the faster time constant τ_{d1} of a two-exponential fit to the decaying phase of the tail current. In representative mutants a rough "limiting slope" measurement of gating valence was also made, and estimates of reversal potential were made from tail currents from each mutant construct. The parameters obtained from each mutant are shown in Table I and are described in detail below.

Mutations at the NH_2-terminal End Show Small Effects on Voltage Dependence and Kinetics of Activation

The acidic residues E333, E334, E335, and D336 form the NH_2-terminal end of the linker in *Shaker*. As can be seen in Fig. 1, all *Shaker*-related mammalian K^+ channels, except Kv1.4, have one or two acidic residues within these four positions. We tested the influence of these charged residues by either deleting them or by reversing the charge with lysine residues, either one at a time or simultaneously. The deletions had little effect on the voltage dependence of activation, but there was a trend

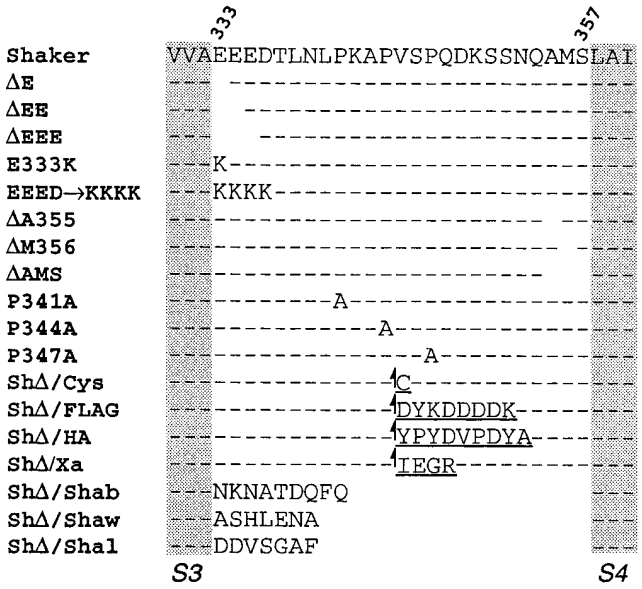

FIGURE 2. Mutations of the *Shaker* S3-S4 region. The wild-type *Shaker* sequence (top) is compared with the sequences of mutations studied here. Mutations included the deletion and charge-reversal of acidic residues at the NH_2-terminal end, deletions at the COOH-terminal end, and substitutions of each of the three proline residues with an alanine. In the insertion mutations (ShΔ/Cys, ShΔ/FLAG, ShΔ/HA, ShΔ/Xa) the underlined sequences were inserted following proline 344, as indicated by the upward arrows. In the final three mutations, the entire S3-S4 linker was replaced with shorter segments from Shab11, Shaw2, or Shal2, respectively (Butler et al, 1990). Dashes indicate amino acid identity to the *Shaker* sequence and blank spaces indicate gaps.

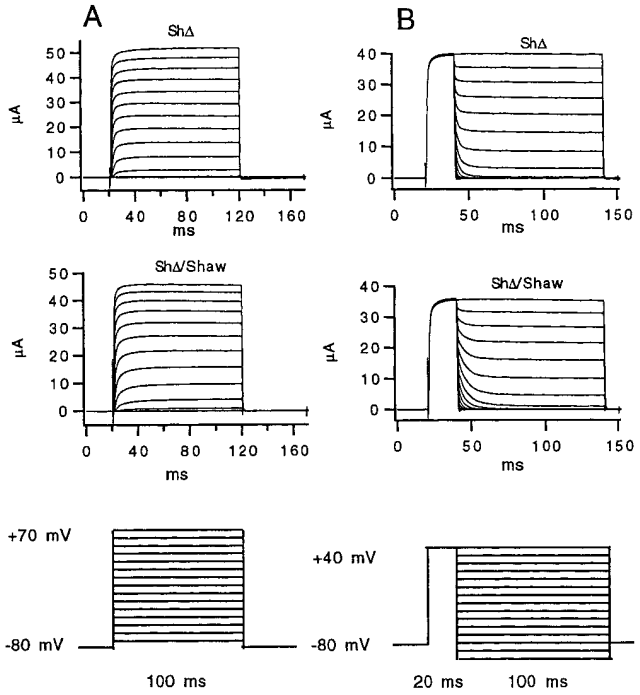

FIGURE 3. Whole-oocyte voltage-clamp protocols and currents from oocytes expressing the "wild-type" ShΔ and the ShΔ/Shaw chimeric channels. (*A*) Activation protocol. Depolarizations of 100-ms duration are given from a holding potential of −80 mV. (*B*) Deactivation protocol. After a 20-ms prepulse to +40 mV, tail currents are measured during 100-ms test pulses at potentials between −100 and +40 mV. Potentials are varied in steps of 10 mV, and pulses are applied at 5-s intervals.

toward faster activation at negative potentials with the single deletion ΔE (Fig. 4 *A*). The average shifts in the activation voltage V_a were between −7 and −11 mV (Table I), which is in the opposite direction from that expected if the neutralization of these acidic residues simply affects the surface charge at the extracellular surface.

The charge reversal E333K also resulted in a −7 mV shift in activation. The reversal of all four charges in the EEED → KKKK mutant produced a +5 mV shift in both steady-state activation and the time constant curves (Fig. 4 *B*); this small shift is in the direction expected for a surface charge effect.

Deletions at the COOH-terminal End Tend to Slow the Rates of Channel Activation

The COOH-terminal ends of the linkers in *Shaker* and its mammalian homologues have four identical amino acid residues (QAMS), except for the presence of threonine in place of M356 in Kv 1.1 (Fig. 1). Deletion of M356 alone shifted the mean voltage of activation by −12 mV when compared to the wild-type channel. The ΔAMS mutant showed a mean activation voltage close to that of the wild type (Table I), although the slope of activation increased. The ΔA and ΔAMS mutants increased the activation time constant at depolarized voltages (Fig. 4 *C*). A comparison of activation time courses at −20 mV (Fig. 5) demonstrates the slowing of activation by these deletions.

Mutations in the Middle of the Linker Did Not Have Appreciable Effects

The *Drosophila Shaker* has a proline-rich sequence (P-X-X-P-X-X-P) in the center of the S3-S4 linker, which is absent in the linkers of the *Shaker*-related mammalian channels and in the other K^+ channel subfamilies. Proline is known to be a helix-breaker, and in multiples it appears predominantly in flexible regions of proteins (MacArthur and Thornton, 1991; von Heijne, 1991). We tested the effect of substituting each of the proline residues with alanine, one at time. The results showed that none of the substitutions resulted in an alteration in the channel activation voltage and little effect on kinetics (Fig. 6 *A* and Table I).

Inserting a Cys Slows Channel Activation

Neither *Shaker* nor its higher homologues has a cysteine residue in the S3-S4 linker. Inserting a Cys after Pro 344

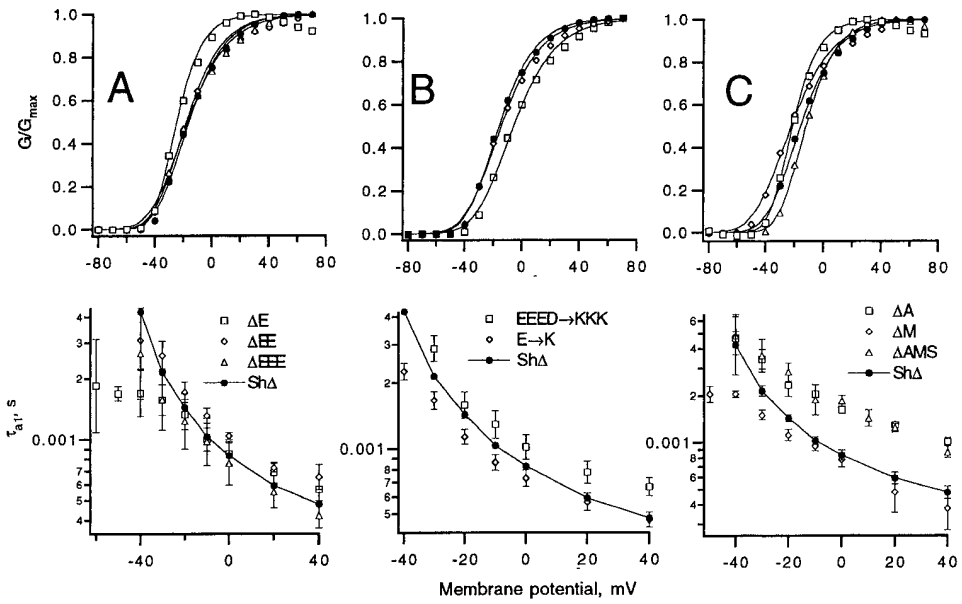

FIGURE 4. Voltage dependence of activation and time constants. Normalized conductance-voltage (*G-V*) curves, and voltage dependence of activation time constant are shown for ShΔ and various mutants: (*A*) deletions at the NH_2-terminal end of the linker; (*B*) charge reversals at the NH_2-terminal end; (*C*) deletions at the COOH-terminal end. G-V curves (*top*) are shown for individual oocytes, chosen to have V_a and k_a values near the medians of 4–10 recordings. The conductance values were computed from the average current during the second half of 100-ms depolarizations to the given voltages and are shown fitted to the fourth power of a Boltzmann function. Time constant τ_{a1} of the predominant component of the activation time course (*bottom*) is plotted as the geometric mean ± SE for n = 5–7 determinations as a function of depolarizing voltage. Lines connect the values for ShΔ (*filled circles*).

did not affect the voltage dependence of activation, but the insertion did slow the time course of activation at depolarized potentials. The mean τ_{a1} at potentials between 0 and +40 mV was about twofold greater than that of the wild type (Fig. 6 *B*), but the deactivation time constant τ_{d1} remained unchanged. Application of 1 mM dithiothreitol either before or during the recording did not change the amplitude or kinetics of the current.

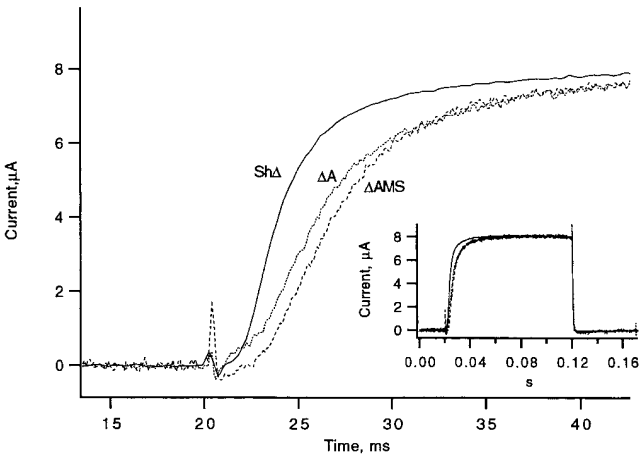

FIGURE 5. Comparison of the time course of activation of ShΔ and the ΔA and ΔAMS mutants. Depolarizations to −20 mV were applied from a holding potential of −80 mV; the entire time courses are shown in the inset. The ΔA and ΔAMS current recordings were scaled by factors of 1.57 and 2.54 to match the steady-state current in the ShΔ recording.

Lengthening of the Linker by Addition of Short Peptide Tags Was Tolerated

The mutant channels with epitopes expressed very well and caused only small alterations in the channel's electrophysiological properties. Their activation voltages and kinetics were close to that of the wild type. However, both the HA and the Factor X_a mutants showed a slight reduction in the slope of activation (Fig. 6 *B* and Table I).

Swapping the Linker Caused Larger Changes in Channel Kinetics

The relatively long *Shaker* linker (25 amino acids) was replaced with the much shorter linkers from *Shab* (9 amino acids), *Shaw* (7 amino acids), and *Shal* (7 amino acids). The *Shab* and *Shaw* linkers resulted in a three- to fourfold slowing of activation throughout the voltage range (Fig. 6 *C*), and produced −13 and +7 mV shifts, respectively. The *Shal* chimera showed a shift of +10 mV but little change in kinetics.

The kinetic effects of these linker substitutions can be seen in the activation and deactivation time courses of Fig. 7, *A* and *B*. Whereas the *Shal* linker results in time courses indistinguishable from wild type, channels with *Shab* and *Shaw* linkers activate and deactivate more slowly. The deactivation time constants (Fig. 7 *C*) are also about threefold larger in these mutants. These effects are in contrast to the effect of the Cys insertion, where the activation time course is slowed but deactivation is as rapid as wild type (Fig. 7, *A* and *B*).

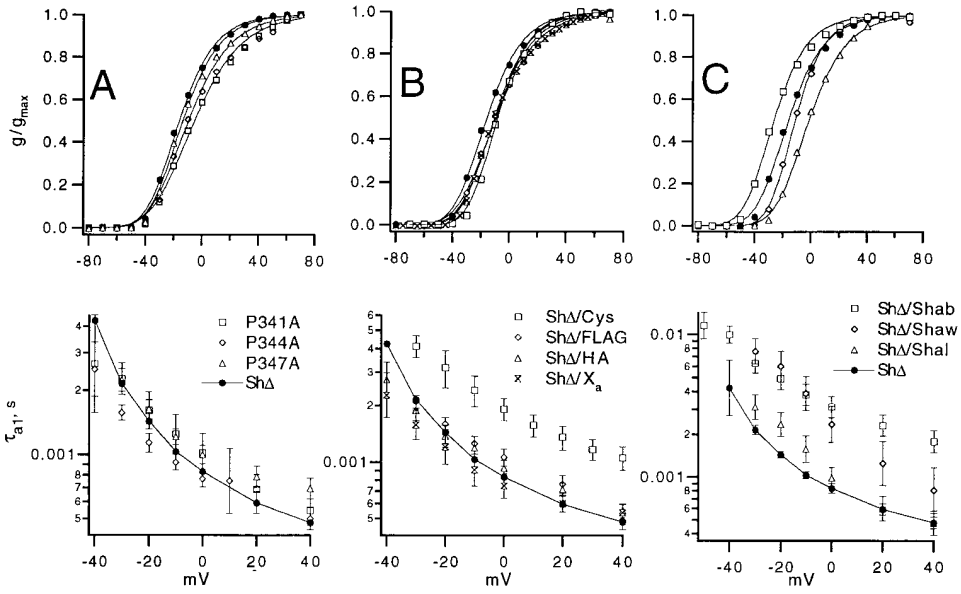

FIGURE 6. Voltage dependence of activation and time constants of mutants. (*A*) Proline substitutions; (*B*) insertions; (*C*) linker sequence substitutions. *G-V* curves (*top*) and time constants (*bottom*) are plotted as in Fig. 4. Error bars represent standard errors with $n = 5$–7.

No Evidence for a Change in Gating Valence

The voltage sensitivity of channel opening, measured at negative potentials where the open probability is low, yields a lower-bound estimate on total channel gating charge (Almers 1978; Hirschberg et al., 1995). With the two-microelectrode voltage clamp we were able to make reliable measurements of channel activation only down to open probabilities $p_o \sim 10^{-2}$. Nevertheless, we computed the apparent gating charge as a rough measure to check whether any of the various classes of mutations resulted in a large change in the limiting voltage sensitivity. Fig. 8 *A* shows activation data from a ShΔ oocyte; Fig. 8 *B* shows the apparent gating valence z_{app} computed according to:

$$z_{app} = \frac{kT}{e_0}\frac{d\ln G}{dV}, \qquad (2)$$

and plotted as a function of the steady-state conductance *G*. For consistency we evaluated z_{app} in each oocyte at the potential where *G* is 1% of its maximum value. The values so obtained are much less than the expected asymptotic value of ~13, but are expected to show any large changes in total gating charge or other effects on the gating mechanism. For all the mutants, these values were close to the value of 6.0 obtained for ShΔ (Table I).

Selectivity Was Not Altered by the Mutations

To evaluate a possible change in the selectivity for K^+ over Na^+ ions, we estimated the reversal potentials in tail-current experiments. Because of the limited speed of the two-microelectrode voltage clamp, clear reversal of the current was not always seen. With the ND 96 bath solution containing 2 mM KCl and 96 mM NaCl, the ShΔ channel had an apparent reversal potential of −85 mV. In all but two of the mutants, reversal potentials were observed in the range −75 to −89 mV (means of 2–7 oocytes where current reversal could be recorded). For the ΔA and ΔE mutants the reversal was more difficult to detect, but nevertheless appeared to be in the

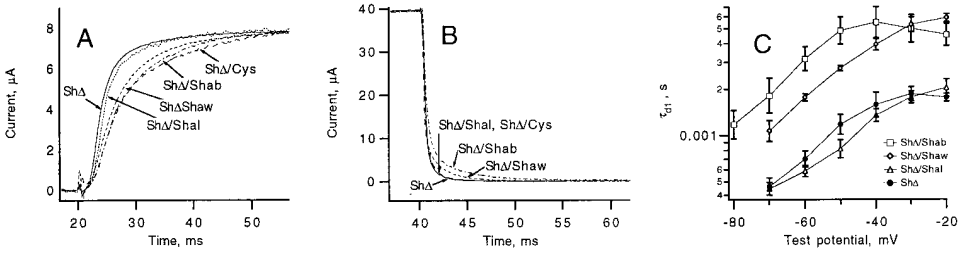

FIGURE 7. Activation and deactivation in chimeric channels. (*A*) Time courses of activation during a −20-mV depolarization for ShΔ, ShΔ/Shal, ShΔ/Shaw, and ShΔ/Shab currents, and for the cysteine insertion mutant ShΔ/Cys. Currents in the mutant constructs were scaled by factors of 0.9, 5.0, 1.0, and 2.17, respectively, to match the ShΔ currents. (*B*) Deactivation time courses at −60 mV after a prepulse to +40 mV. Currents from ShΔ/Shal, ShΔ/Shaw, and ShΔ/Shab were scaled by factors of 1.5, 0.78, 1.45, and 1.25, respectively. (*C*) Voltage dependence of the predominant time constant of deactivation, τ_{d1}, as a function of test potential for ShΔ and the chimeric channels. Plotted are the geometric means ± SE ($n = 6$).

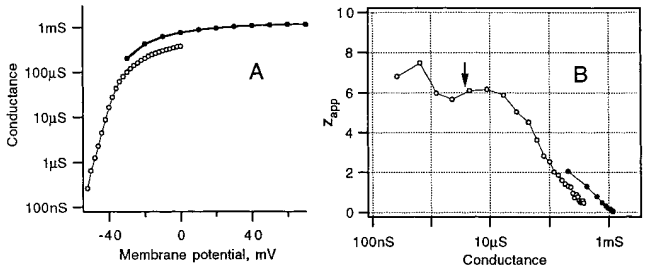

FIGURE 8. Determination of apparent gating valence z_{app}. (*A*) Conductance-voltage curve. Mean current from ShΔ channels during the second half of 400-ms depolarizations from −80 mV were converted to conductance and plotted as open circles as a function of voltage; conductances obtained from shorter (100 ms), larger depolarizations are plotted as filled circles. (*B*) Values of z_{app}, computed as the logarithmic derivative of *G* with respect to voltage according to Eq. 2 are plotted as a function of *G* as in Zagotta et al. (1994). Because of growing errors at lower conductances, we took the estimate of z_{app} to be the value at 1% of the maximal conductance, as indicated by the arrow.

same voltage range. The similarity of reversal potentials is consistent with there being no change in the selectivity due to mutations in the S3-S4 linker.

DISCUSSION

Our goal in the present study was to investigate the role of the S3-S4 linker region in the activation of the *Shaker* K^+ channel. The results are interesting in two respects. First, the effects of mutations on the voltage dependence of activation were surprisingly small. Despite the proximity of this extracellularly disposed region to the S4 region, which has been implicated as an important part of the voltage sensor, large changes in charge and in the length of the S3-S4 linker produced only minor changes in the voltage dependence of activation. Voltage shifts were at most 13 mV in magnitude, and changes in other measures of voltage sensitivity were similarly small. Second, the main effect of some mutations, including the replacement of the 25-residue *Shaker* sequence with the 9 and 7-residue *Shab* and *Shaw* linkers, were changes in the speed of activation and deactivation. It is interesting that these kinetic effects occurred in the absence of large changes in the voltage dependence of activation.

Structure of the S3-S4 Linker

An examination of the linker sequence within the members of the four different K^+ subfamilies reveal some notable features (see Fig. 1). First, in *Shaker* and its mammalian homologues the linker shows greater variation in length and composition than it does in the members of the *Shab*, *Shaw* and *Shal* subfamilies. The *Drosophila Shaker* linker is the longest (25 amino acid residues) and except for a few identical amino acids or conservative substitutions at the NH_2- and the COOH-terminal ends, it is quite different than the mammalian linkers, which are much shorter and have a preponderance of glycine and glutamine residues.

The shorter (7 to 9 residue) linkers in the *Shab*, *Shaw*, and *Shal* subfamilies are strikingly well conserved across the different members. The *Drosophila Shal* linker is essentially identical to its rat, mouse, and human counterparts. The linkers within the mammalian *Shab*-related sequences are also identical to each other, and the *Drosophila Shab* linker is related to these in having five identical residues out of the total nine and has one conservative substitution. A potential N-glycosylation consensus site in this linker is conserved across all *Shab* members and species. The linkers within the members of the *Shaw*-like mammalian subfamily too are nearly identical; however the *Drosophila* linker matches poorly, having only one identical residue and three conservative substitutions out of a total of seven residues. Evidently, the S3-S4 linkers do not represent a collection of random sequences, but form groups of related sequences, which are characteristically specific for each of the four subfamilies; some even have conserved glycosylation sites.

Effects on the Voltage Dependence of Activation

We created several different types of mutations in the *Shaker* linker and performed an initial characterization of their effects on channel activation, using the two-microelectrode voltage clamp technique. The results showed that these mutations had at most moderate effects on the voltage dependence of activation. Evidently, the linker does not form a part of the voltage-sensor of the channel, despite its proximity to S4. The small effects from the deletion or charge reversal of the residues most distant in the sequence from S4, the acidic residues E333, E334, E335, and D336, suggest that they are physically distant from the voltage-sensing moieties of the channel. The substitutions of each of the proline residues with an alanine also had no effect on the voltage dependence or the kinetics, even though the proline triplet repeat would be expected to contribute to the flexibility of the linker. Elongating the linker by adding several different types of short peptide epitopes also did not affect the voltage dependence of activation or the kinetics significantly. The FLAG peptide is very hydrophilic in its composition (7 of its 8 residues are either acidic or basic), while the HA peptide would increase the hydrophobicity in the linker. The results with these peptides suggest that the polarity of the linker's environment does not change in the course of channel gating. It will be interesting to test for a change in the accessibility of the linker in situ from the external surface either by using the monoclonal antibody against

the HA peptide, as has already been done in the case of a FLAG epitope by Shih and Goldin (1995), or by enzymatic cleavage of the linker by enterokinase and Factor X_a protease.

Kinetic Effects of Mutations

Certain of the mutations affected the time course of activation of the macroscopic ionic currents. Deletion of one or more of the residues at the conserved COOH-terminal end of the linker, introduction of a single Cys residue, or swapping the *Shaker* linker with the short linker segment from either the *Shab* or the *Shaw* subfamily of voltage-gated K^+ channels slowed the rates of activation at all depolarizing potentials. Recent studies have shown that the position M356 can be accessed from the outside at both resting and depolarized membrane potentials (Larsson et al. 1996; Mannuzzu et al. 1996). Our results show that deletion of the adjacent A355 alone or with two neighboring residues (ΔAMS) increase the activation time constant with only small effects on the voltage dependence, whereas deletion of M356 alone slightly decreases the time constant of activation and shifts the activation voltage. Thus the residues which are closest to S4 seem to be important in affecting the rate of one or more transitions leading to the opening of the channel; however the surprising effect of the Cys insertion in the middle of the linker suggests that other interactions may also be present.

Chimeric channels (ShΔ/Shab and ShΔ/Shaw) produced a larger slowing of channel activation (three- to fourfold increase in τ_{a1}), whereas the ShΔ/Shal chimera had little kinetic effect. Deactivation kinetics were also slower for the channels with the *Shab* and *Shaw* linkers, although the *Shal* linker, being like *Shaw* only seven residues in length, yielded normal deactivation kinetics. It is interesting that the changes in kinetics were accompanied by only small shifts in voltage dependence. This is in contrast to the effects of most mutations that affect *Shaker* activation, where kinetic changes are typically accompanied by large voltage shifts. The origin of the kinetic effects of the mutations studied here is unclear. One explanation is that the mutations may affect the stability of intermediate conformations that are visited during the activation process. The long delay in the time course of activation of the channels implies that there are many such intermediate states (Zagotta et al., 1994). The interactions that would allow the mutations to affect the stability of intermediates are unknown, but it should be kept in mind that two- to fourfold changes in rates represent small free-energy differences, and would reflect rather weak interactions.

Wei et al. (1990) showed that the four voltage-gated K^+ subfamilies in Drosophila differed in the rates of activation of their macroscopic currents, in the order *Shaker* > *Shal* > *Shaw* > *Shab* and spanning an overall range of 16-fold. Though on a reduced scale, our chimeras follow the same rank order of changes in activation rates (Fig. 6 *C*). It appears that in the chimeric channels the S3-S4 linker partially confers the parental channel type's kinetics on *Shaker*. This suggests a possible role of the linker in establishing the time scale of activation of the channels. A similar conclusion has been reached from studies of L-type Ca^{2+} channel chimeras (Nakai et al, 1994), where substitution of the S3-S4 linker of Domain 1 conferred the kinetic phenotypes of skeletal muscle and cardiac Ca^{2+} channels.

Structural Implications

Residues in the S4 region appear to constitute most of the gating charge in *Shaker* potassium channels (Aggarwal and MacKinnon, 1996; Seoh et al., 1996). Accompanying the voltage-dependent gating charge movement are conformational changes that dramatically alter the accessibility of S4 residues to the inner and outer membrane surfaces in *Shaker* channels (Larsson et al., 1996) and in Domain 4 of sodium channels (Yang et al., 1996). This apparent translocation of several residues from the inner to the outer membrane surface upon depolarization can explain much of the observed charge movement, ~4 e_0 per subunit in magnitude. A popular model for the underlying conformational change is a helical-screw motion of an alpha-helical S4 region (Catterall, 1986; Durell and Guy, 1992). In this model some 20 Å of displacement would be required to translocate four charges, requiring that the S3-S4 linker be highly flexible. The *Shaker* S3-S4 linker, being relatively long and having multiple proline residues, seems well suited for this function. However, the linkers in the other potassium channel subfamilies are much shorter; in mammalian sodium channels the linkers are also very short, only 4–9 residues in length (Goldin, 1995). Do the shorter linkers preclude a large S4 translation? Molecular modelling by Dr. T.B. Woolf (personal communication) shows that the 7-residue *Shab* linker is sufficiently long to substitute for the *Shaker* linker the model of Durell and Guy in its "closed" and "open" states. Even with the *Shab* linker, no change in secondary structure of S3 or S4 is required between these states.

The large movement of the S3-S4 linker in the helical-screw model nevertheless would predict that alterations in the linker sequence would result in substantial differences in the free-energy difference ΔG for channel opening. The largest voltage shift (13 mV) induced by our mutations corresponds to a $\Delta\Delta G$ of at most 1.2 kcal/mole. This value is calculated from the electrostatic energy shift $q\Delta V$, where q is the total gating charge of 4.3 e_0 per subunit. The small $\Delta\Delta G$ suggests that the linker undergoes little if any conformational change in the process of gating. This is consistent with alternative views of S4 motion, in which it undergoes

state-dependent movements or secondary structure changes that leave the S3-S4 region unaffected. A scheme involving secondary structure changes in S4 was proposed by Guy and Conti (1990) to allow charge movement without requiring linker motion. A more recent proposal of a helix-to-loop rearrangement of S4 (Aggarwal and MacKinnon, 1996), which could also leave the S3-S4 linker largely stationary, becomes plausible in view of the very large peptide translocations that occur in voltage-dependent gating of colicin IA (Slatin et al., 1994; Qiu et al., 1996).

We thank Dr. Tom Woolf (Johns Hopkins University) for his insights from molecular modelling.
This work was supported by National Institutes of Health grant NS21501.

Original version received 5 September 1996 and accepted version received 13 November 1996.

REFERENCES

Aggarwal, S.K., and R. MacKinnon. 1996. Contribution of the S4 segment to gating charge in the *Shaker* K^+ channel. *Neuron.* 16: 1169–1177.

Almers, W. 1978. Gating currents and charge movements in excitable membranes. *Rev. Physiol. Biochem. Pharmacol.* 82:96–190.

Bezanilla, F., and C.M. Armstrong. 1977. Inactivation of the sodium channel. I. Sodium current experiments. *J. Gen. Physiol.* 70:549–566.

Blumenthal, E.M., and L.K. Kaczmarek. 1992. Modulation by cAMP of a slowly activating potassium channel expressed in Xenopus oocytes. *J. Neurosci.* 12:290–296.

Butler, A., A. Wei, and L. Salkoff. 1990. *Shal*, *Shab* and *Shaw*: three genes encoding potassium channels in Drosophila. *Nucleic Acids Res.* 18:2173–2174.

Catterall, W.A. 1986. Molecular properties of voltage-sensitive sodium channels. *Annu. Rev. Biochem.* 55:953–985.

Chandy, K.G., and G.A. Gutman 1994. Voltage-gated K^+ channels. *In* Ligand and Voltage-gated Ion Channels. R.A. North, editor. CRC Press, Boca Raton, FL. 1–71.

Deng, W.P., and J.A. Nickoloff. 1992. Site-directed mutagenesis of virtually any plasmid by eliminating a unique site. *Anal. Biochem.* 200:81–88.

Durell, S.R., and H.R. Guy. 1992. Atomic scale structure and functional models of voltage-gated potassium channels. *Biophys. J.* 62: 238–247.

Goldin, A. 1995. Voltage-gated sodium channels. *In* Ligand- and Voltage-gated Ion Channels. R.A. North, editor. CRC Press, Boca Raton, FL. 73–111.

Guy, H.R., and F. Conti. 1990. Pursuing the structure and function of voltage-gated channels. *Trends Neurosci.* 13:201–206.

Hirschberg, B., A. Rovner, M. Lieberman, and J. Patlak. 1995. Transfer of twelve charges is needed to open skeletal muscle Na channels. *J. Gen. Physiol.* 106:1053–1068.

Hoshi, T., W.N. Zagotta, and R.W. Aldrich. 1990. Biophysical and molecular mechanisms of Shaker potassium channel inactivation. *Science (Wash. DC).* 250:533–538.

Kamb, A., J. Tseng-Crank, and M.A. Tanouye. 1988. Multiple products of the Drosophila *Shaker* gene may contribute to potassium channel diversity. *Neuron.* 1:421–430.

Kast, C., V. Canfield, R. Levenson, and P. Gross. 1995. Membrane topology of P-glycoprotein as determined by epitope insertion: transmembrane organization of the N-terminal domain of mdr3. *Biochemistry.* 34:4402–4411.

Larsson, H.P., O.S. Baker, D.S. Dhillon, and E.Y. Isacoff. 1996. Transmembrane movement of the *Shaker* K^+ channel S4. *Neuron.* 16:387–397.

MacArthur, M.W., and J.M. Thornton. 1991. Influence of proline residues on protein conformation. *J. Mol. Biol.* 218:397–412.

Mannuzzu, L.M., M.M. Moronne, and E.Y. Isacoff. 1996. Direct physical measure of conformation rearrangement underlying potassium channel gating. *Science (Wash. DC).* 271:213–216.

Nakai, J., B.A. Adams, K. Imoto, and K.G. Beam. 1994. Critical roles of the S3 segment and S3-S4 linker of repeat I in activation of L-type calcium channels. *Proc. Natl. Acad. Sci. USA.* 91:1014–1018.

Pfaff, S.L., M.M. Tamkun, and W.L. Taylor. 1990. pOEV: a Xenopus oocyte protein expression vector. *Anal. Biochem.* 188:192–199.

Qiu, X.-Q., J.K.S., P.K. Kienker, A. Finkelstein, and S.L. Slatin. 1996. Major transmembrane movement associated with colicin Ia channel gating. *J. Gen. Physiol.* 107:313–328.

Ray, F.A., and J.A. Nickoloff. 1992. Site-specific mutagenesis of almost any plasmid using a PCR-based version of unique site elimination. *Biotechniques.* 13:342–346.

Schoppa, N.E., K. McCormack, M.A. Tanouye, and F.J. Sigworth. 1992. The size of gating charge in wild-type and mutant Shaker potassium channels. *Science (Wash. DC).* 255:1712–1715.

Schwarz, T.L., B.L. Tempel, D.L. Papazian, Y.N. Jan, and L.Y. Jan. 1988. Multiple potassium-channel components are produced by alternative splicing at the Shaker locus of Drosophila. *Nature (Lond.).* 331:137–142.

Seoh, S.-A., D. Sigg, and F. Bezanilla. 1996. Voltage-sensing residues in the S2 and S4 segments of the *Shaker* K^+ channel. *Neuron.* 16:1159–1167.

Shih, T.M., and A.L. Goldin. 1995. Use of hydrophilic amino acid epitope insertions to probe the topology of the Shaker H4 potassium channel. *Biophys. J.* 68:266*a*. (Abstr.).

Sigworth, F.J. 1994. Voltage gating of ion channels. *Q. Rev. Biophys.* 27:1–40.

Slatin, A., X.Q. Qiu, K.S. Jakes, and A. Finkelstein. 1994. Identification of a translocated protein segment in a voltage-dependent channel. *Nature (Lond.).* 371:158–161.

von Heijne, G. 1991. Proline kinks in transmembrane alpha helices. *J. Mol. Biol.* 218:499–503.

Wearne, S.J. 1990. Factor Xa cleavage of fusion proteins. Elimination of non-specific cleavage by reversible acylation. *FEBS Lett.* 263:23–26.

Wei, A., M. Covarrubias, A. Butler, K. Baker, M. Pak, and L. Salkoff. 1990. K^+ current diversity is produced by an extended gene family conserved in *Drosophila* and mouse. *Science (Wash. DC).* 248: 599–603.

Yang, N., A. George, Jr., and R. Horn. 1996. Molecular basis of charge movement in voltage-gated sodium channels. *Neuron.* 16: 113–122.

Zagotta, W.N., T. Hoshi, J. Dittman, and R.W. Aldrich. 1994. Shaker potassium channel gating. II. Transitions in the activation pathway. *J. Gen. Physiol.* 103:279–319.

Zhong, M., L. Lin, and N.R. Kallenbach. 1995. A method for probing the topography and interactions of proteins. Footprinting of myoglobin. *Proc. Natl. Acad. Sci. USA.* 92:2111–2115.